17th World Conference on Earthquake Engineering, 17WCEEE
Sendai, Japan - September 27th to October 2nd 2021

A SET OF RULES FOR CHOOSING FAULT PLANES IN REAL-TIME POST-EVENT EARTHQUAKE LOSS ASSESSMENTS

M. Ordaz [1], M.A Salgado-Gálvez[2], B. Huerta[3], S.K. Singh[4], X. Pérez-Campos[5]

[1] *Professor, Instituto de Ingeniería, UNAM, mordazs@iingen.unam.mx*
[2] *Earthquake hazard and risk specialist, ERN, mario.sal.gal@gmail.com*
[3] *Engineering models manager, ERN, benjamin.huerta@ern.com.mx*
[4] *Professor, Instituto de Geofísica, UNAM, krishnamex@yahoo.com*
[5] *Professor, Instituto de Geofísica, UNAM, xyoli@geofisica.unam.mx*

Abstract

Rapid post-earthquake loss assessments require as input the ground motion footprint of the event. These footprints describe the geographical distribution of the seismic intensities which, at the same time, depend on the characteristics of the event such as its magnitude, location, depth, focal mechanism and orientation of the fault plane. For most earthquakes with $M_W \geq 5$, moment tensor solution and, hence, the characteristics of the two nodal-planes are available. This study proposes a simple set of rules for choosing the likely fault plane from the two nodal planes, based on a previous characterization of the seismic sources in the area under study that are commonly used in probabilistic seismic hazard analyses. With the selection of the fault plane, a critically required information for generating the parametric ground motion footprint is at hand in a matter of minutes to be later used in a loss assessment stage. These almost real-time loss assessments are useful for different disaster risk management activities ranging from emergency planning and management to the definition of triggers for parametric insurance instruments. The application of this methodology is illustrated for a historical earthquake in Guatemala, where loss results at country level are highly sensitive to the selection of the correct nodal plane as the fault plane, showing that the proposed rules yield congruent results with the observed and recorded ground motions.

Nodal planes; earthquake risk; real-time loss assessment; parametric insurance

17th World Conference on Earthquake Engineering, 17WCEE
Sendai, Japan - September 27th to October 2nd 2021

1. Introduction

In the aftermath of an earthquake, there is an increasing need of having estimations of the ground motion intensities in the affected areas, to be used in rapid post-earthquake loss assessments. These risk assessments can provide, in a matter of minutes, valuable information for: (a) emergency planning and management, such as a preliminary estimation of injuries and fatalities; and (b) identification of areas with more collapsed buildings, so that personnel and machinery can be timely deployed to them, as well as blocked roads because of debris, so that ambulances can find optimal paths to and from hospitals. In addition, and more recently, parametric insurance instruments have been designed so that based on an almost real-time assessment of the earthquake losses the decision can be made of whether a pay-out occurs. Furthermore, transparency is needed in the estimation of all components of the risk assessment process (i.e., hazard, exposure and vulnerability). Hence, a pre-established set of rules for the selection of the appropriate fault plane is not only useful but desirable.

Parametric ground motion footprints can be generated in a matter of seconds in probabilistic seismic hazard analysis (PSHA) programs such as R-CRISIS [1], using as input data some basic source information such as the magnitude, location and depth, along with parameters that characterize the type of faulting and orientation of the fault plane (strike, dip, and rake) and one or more ground motion prediction equations (GMPE). International agencies, such as the National Earthquake Information Center (NEIC) of the U.S. Geological Survey (USGS) provide magnitude, location, and depth of earthquakes. The NEIC solutions are available within a very short time. Also, for most $M_W \geq 5$ earthquakes, NEIC reports the centroid moment tensor (CMT) solution and the two nodal planes, assuming a double-couple source. The CMT solution is also published by the Global Centroid Moment Tensor Project of Columbia University. As this solution is based on larger dataset, it is available later than the NEIC solution.

A nodal plane (NP) is characterized by its azimuth (φ), dip (δ), and rake (λ) (see Aki and Richards, [2] for the convention). One of the two NPs reported in the CMT solution is the fault plane. The correct selection of the fault plane is critical for the reliable estimation of the geographical distribution of the ground motion intensities and the subsequent earthquake loss assessment. For large events, the failure to select the correct fault plane may result in an under- or over-estimation of the consequences of the event that, for the previously mentioned disaster risk management purposes, may be highly misleading. This paper proposes a simple set of rules for choosing the more likely fault plane based on the CMT solution.

The proposed set of rules are intended to be used in areas where PSHA have been conducted previously, so that a subdivision of the region in seismic provinces is available. Based on the reported location and depth, the event is assigned to a unique seismic province from where the shape characteristics of the rupture area are designated (e.g., rectangular or elliptical area and the aspect ratio); its orientation is governed by the chosen fault plane resulting from the application of the proposed rules. Finally, making use of the previously assigned GMPE of the source, the ground motion intensities are obtained.

To highlight the relevance of the proposed set of rules, the comparison of direct losses at country level is made considering both NPs of the 1976 Guatemala and the 2017 Tehuantepec earthquakes. The earthquake risk assessment is performed in R-CAPRA using openly available exposure and vulnerability datasets.

2. Characterization of seismic provinces and sources

To develop a set of rules that permits the selection of the more likely fault plane automatically, we first require knowledge of the characteristics of the fault plane at each seismic province.

We note that the division of a region in seismic provinces for PSHA relies heavily on seismicity and seismotectonics, with plate tectonics providing the basic framework. This division is facilitated by plotting the seismicity and available focal mechanisms of the region. As an example, let us consider a region that includes Mexico, Central America, and the Caribbean. The seismicity, taken from the GEM catalog [3] and color-coded according to the source depth, is illustrated in Figure 1a. Figure 1b shows a similarly color-coded plot of the focal mechanisms extracted from the Global CMT catalog. The Middle America Trench (MAT) where Cocos Plate begins subduction below the North American Plate is marked. These two figures, and the vast literature on subduction process, seismicity, and seismotectonics of the region, along with geologically mapped faults, provide the necessary information for the division. A seismic province is constructed such that it encloses earthquakes of similar focal mechanisms and level of seismicity. We note that in some provinces, the seismicity is very low and no focal mechanism solution is available. The region shown in Figure 1 has been divided in 152 seismic provinces [4] using existing zonations for the domain under study [5, 6, 7, 8]. The provinces are shown in orange polygons in Figure 1. The main provinces and the associated characteristics of the expected faulting in them are:

1. Coupled plate interface along the subduction zone (shallow-dipping thrust faulting at the interface with strike, φ, roughly parallel to the trench).
2. Subducted slab (normal faulting with strike, generally, parallel to the trench).
3. Outer rise, offshore from the trench (normal faulting with strike, generally, parallel to the trench).
4. Forearc crust (often normal faulting, with strike parallel to trench).
5. Volcanic arc crust (normal faulting with strike, generally, parallel to the trench).
6. Pacific – North America and Pacific – Rivera plate boundaries (strike-slip and normal faulting earthquakes, azimuth of the fault plane parallel to the plate boundary.
7. Caribbean - North America plate boundary (strike-slip faulting with azimuth parallel to the plate boundary).

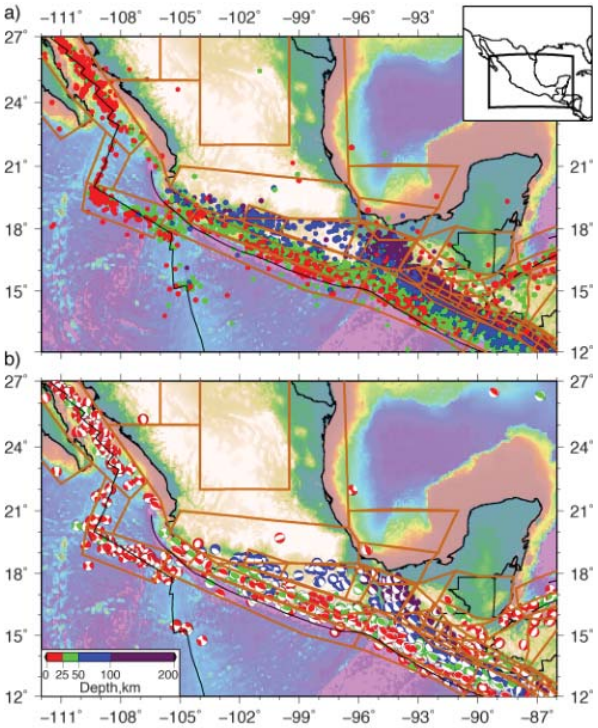

Fig. 1 – a) Seismicity of Mexico, Central America and the Caribbean from the ISC-GEM catalog, 1900-2011; b) Focal mechanisms reported in GCMT catalog, 1976-2015. The depths of the events are color-coded

3. Selection of the fault plane

As mentioned above, the seismic provinces defined for PSHA enclose earthquakes of similar focal mechanisms. The rules for automatic selection of the correct nodal plane as the fault plane is facilitated by statistical analysis of the parameters of the reported mechanisms. This, of course, is possible only for seismic provinces in which several focal mechanism solutions are available. For these provinces, we performed a statistical analysis on φ, δ, and λ of both NPs. As examples, we present analysis of a selected seismic province and provide the results for other two:

(a) Caribbean - North America plate boundary

Along the Caribbean - North America plate boundary we expect, in general, strike-slip faulting. The nodal plane parallel to the plate boundary is the likely fault plane. As an example, let us consider the Guatemala Earthquake of 4 February 1976, M_W7.5, which ruptured the Motagua Fault. The plate boundary in the region has an azimuth of about N60°E. For this event, the two NPs listed in the GCMT catalog are:

NP1: φ = 254°, δ = 73°, λ = -10°
NP2: φ = 347°, δ = 80°, λ = -162°

Since the azimuth of NP1 is consistent with that of the plate boundary in the region, it is likely to be the fault plane. This is confirmed by field observations [9].

We note that in the strike-slip domain the fault is often nearly vertical. A slight change in the dip may result in a change of strike by 180°. For this reason, a nodal plane whose azimuth is ~180° from the prescribed azimuth is equally acceptable and the criterion should permit its selection as the fault plane. As an example, consider the nodal planes of an event that occurred on 14 June 2009 (M_W 5.1) near the 1976 earthquake focus. The NPs listed in the GCMT catalog are:

NP1: φ = 5°, δ = 85°, λ = 177°
NP2: φ = 95°, δ = 87°, λ = 8°

The azimuth of NP2 is similar to that of the plate boundary. Therefore, it is the likely fault plane, even though its azimuth is 159° less than that of the 1976 earthquake.

Focal mechanisms and statistics of the nodal-plane parameters of earthquakes in the seismic province that encloses a segment of the Caribbean-North America plate boundary are shown in Figure 2. The plots include the two strike-slip events discussed above. Rakes of 7 out of 8 events correspond to strike-slip faulting. The dip, peaked at ~80°, is relatively high, as expected for a strike-slip faulting.

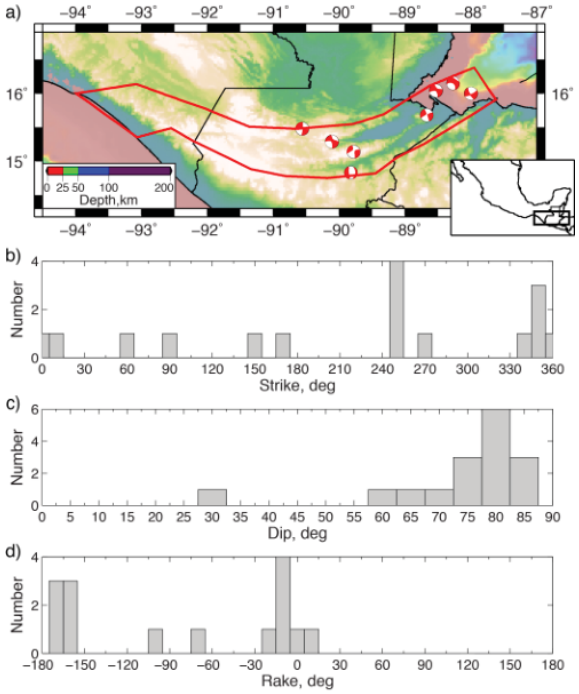

Fig. 2 – a) GCMT focal mechanisms in the Caribean-North America plate boundary seismic province defined by the red polygon. b, c, d) Statistics for strike, dip and rake

(b) Coupled Plate Interface along the Mexican Subduction Zone

Earthquakes in this seismic province are a result of reverse faulting on a shallow-dipping plane. The azimuth of the fault is parallel to the trench. To illustrate a typical focal mechanism of this type of event, let us consider the two NPs, NP1 and NP2, for the 19 September 1985, Michoacan earthquake (M_W8.0) listed in GCMT catalog:

NP1: $\varphi = 301°$, $\delta = 18°$, $\lambda = 108°$
NP2: $\varphi = 106°$, $\delta = 73°$, $\lambda = 85°$

The azimuths of both planes are parallel to the Middle America trench and the rakes, λ, are similar and indicate thrust faulting. The shallow dip, δ, of NP1, however, identifies it as the fault plane.

In this zone there are locations which also include some focal mechanisms that are not consistent with shallow-dipping thrust faulting. The statistics of φ, δ, and λ obtained for this zone indicate a bimodal distribution and the rake distribution is peaked at 90°, indicating that most of them correspond to thrust-faulting events. For these two seismic provinces, the NP characterized by φ of 280° ± 45° is the fault plane. This NP will have δ of 20° ± 10° and rake, λ, of 90° ± 30°. However, requiring only that the azimuth of the NP fall in the range given above yields the correct choice of the fault plane.

(c) Subducted Slab

Most earthquakes within the subducted slab are normal-faulting events, although some steeply-dipping thrust events have also been reported in the subducted Cocos plate near the Pacific Coast of Mexico [10]. The azimuths of the NPs of these intraslab earthquakes are roughly parallel to the trench. The preferred fault plane is the one that dips in the direction of plate subduction. As an example, let us consider the Puebla-

Morelos, Mexico earthquake of 19 September 2017 (M_W7.1) located at a depth of 57 km. The two NPs reported in GCMT catalog are:

NP1: $\varphi = 300°$, $\delta = 44°$, $\lambda = -83°$
NP2: $\varphi = 109°$, $\delta = 46°$, $\lambda = -97°$

Similar to the 1985 Michoacan earthquake, the azimuths of both planes are parallel to the trench. In this case, the dip and the rake of the two planes are similar. However, the requirement that the dip of the fault be in the direction of the subducted slab, favors NP1 as the fault plane as the other plane dips towards the trench.

While the plane dipping in the direction of the plate subduction is usually thought to be the fault plane, this may not necessarily be the case. The source parameters of the 2017 Puebla-Morelos earthquake have been estimated from waveform modelling (see, [11, 12]). Yet these studies were unable to resolve the fault plane. A more illustrative example is provided by a large (M_w 7.8) intermediate-depth earthquake (H=95 km) that occurred the 13 June 2005 in the Tarapaca region in northern Chile. The two NPs reported in GCMT are:

NP1: $\varphi = 353°$, $\delta = 67°$, $\lambda = -94°$
NP2: $\varphi = 182°$, $\delta = 23°$, $\lambda = -81°$

Both azimuths are roughly parallel to the coast. From the criterion above, the preferred fault plane should be NP1. However, detailed studies by Peyrat et al. [13] and Delouis and Legrand [14] suggest that the sub-horizontal nodal plane, NP2, was the fault plane. In this case, our criterion would have selected the wrong NP as the fault plane.

The statistics of φ, δ, and λ obtained for this zone indicate a bimodal distribution. The rake distribution is peaked at -90°, indicating that these are normal-faulting events. Since we assume that the fault plane dips in the direction of plate subduction, the nodal plane characterized by φ of 280° ± 45° is the likely fault plane. This NP has a dip, δ, of 45° ± 15° and rake, λ, of -90° ± 30°.

The discussion above briefly summarizes the reasoning that we have used in developing a set of rules to select the likely fault plane given the two NPs in any seismic province of Mexico, Central America and the Caribbean. These rules are given below:

1. For an earthquake, whose location and depth corresponds to the seismic province of coupled plate interface along the subduction zone, the NP whose azimuth is parallel to the strike of the trench with low dip (~15°) is taken as the fault plane. In the subduction zones of Mexico and Central America, the strike of the trench is between 270° and 320° (or, equivalently, between 90° and 140°).

2. For events located in the subducted-slab seismic province, the NP whose azimuth is parallel to the trench and dips in the direction of the subducted slab is taken as the fault plane.

3. At strike-slip plate boundaries, where strike-slip earthquakes dominate, the NP whose strike is parallel to the plate boundary is taken as the fault plane. In the strike-slip domain the fault is often nearly vertical. A slight change in the dip may result in a change in strike of 180°. For this reason, a plane whose azimuth is ~180° from the prescribed azimuth is equally acceptable as the fault plane.

4. A tolerance of ± 45° in the strike of the chosen fault plane is allowed from the one prescribed in the rule.

5. If the strike is outside this range, then the rake of the event is checked. If the rake corresponds to a reverse fault (i.e., $45° \leq \lambda \leq 135°$), then the plane that corresponds to the smaller dip is chosen. If it is

a normal fault (i.e., $-135° \leq \lambda \leq -45°$), then the NP corresponding to the larger dip is taken as the fault plane.

6. If neither the strike nor the rake criteria are met by the two planes and the earthquake is not in strike-slip dominated source region, then either one of the NPs is taken as the fault plane.

7. For seismic provinces of low seismicity, with no focal mechanisms listed in the GCMT catalog, the selection of fault plane is based on the rake of the NPs. If the rake corresponds to a reverse fault (i.e., $45° \leq \lambda \leq 135°$), then the plane with smaller dip is chosen; if it is a normal fault (i.e., $-135° \leq \lambda \leq -45°$), then the plane corresponding to the larger dip is taken as the fault plane.

It is worth noting that the rules (5) to (7) assume that thrust and normal faulting, generally, occurs on shallower and steeper fault planes, respectively. This may not always be case, an example being the 2005 Terrapaca, Chile earthquake mentioned before.

4. Example

As examples of the application and usefulness of the methodology**,** we consider the highly destructive earthquake of 4 February 1976 Guatemala (M_w7.5) to discuss the importance of the correct selection of the fault plane on the estimation of seismic intensities and the almost real-time post-event loss estimation.

This earthquake killed about 23,000, injured 74,000, and left more than 1 million persons homeless. The tectonic and seismological aspects of the earthquake were studied in detail by Plafker [9] and Kanamori and Stewart [15], respectively. The epicenter of the earthquake given by Kanamori and Stewart is 15.27°N, 89.25°W and waveform analysis reveals an asymmetric bilateral rupture.

The relevant source parameters of the earthquake, reported in the GCMT catalog, are:

Centroid location: 15.14°N, 89.78°W
Depth: 16.3 km
$M_w = 7.5$

NP1: $\varphi = 254°$, $\delta = 73°$, $\lambda = -10°$
NP2: $\varphi = 347°$, $\delta = 80°$, $\lambda = -162°$

We note that the GCMT centroid location is 59 km from the reported epicenter [15] at an azimuth of 256°. While the epicenter falls on the Motagua Fault where ground breakage was reported, the centroid location is about 15 km to the North of the Fault.

Since this earthquake was used in developing the rules, it is no surprise that NP1 is chosen as the fault plane. For a crustal strike-slip earthquake, the expected rupture area is of approximately 3200 km^2, in fairly close agreement with that reported by Plafker [9] and Kanamori and Stewart [15]. Estimated length based on the relationship between L and Mw for strike-slip fault by Wells and Copperfield [16] is 120 km.

4.1 Rapid estimation of seismic intensities and losses

Immediately after an earthquake no information on source directivity and rupture dimension is available. Therefore, the seismic intensities and losses are estimated assuming a bilateral rupture initiating at centroid location and values of L=120 km. The estimations with NP1 and NP2 as fault planes, are shown in Figure 3 where the local site effects have been considered following the parametric approach proposed by Chiou and Youngs [17] based on the Vs30 values.

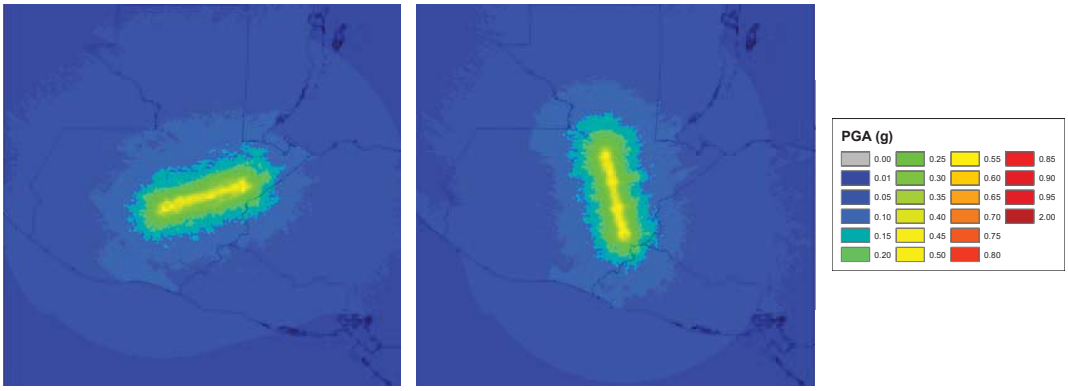

Fig. 3 – Ground motion intensity distributions (in g) with NP1 (left) and NP2 (right) for the 1976 Guatemala Mw7.5 earthquake

Using the exposure and vulnerability datasets for Guatemala of the UNISDR's Global Risk Model [18, 19, and following the methodological proposal by Ordaz [20], implemented in R-CAPRA using a single event approach (see details in [21]), a seismic risk assessment was performed to estimate the direct losses at country level considering the two fault planes. This exposure database accounts only for buildings of different types (i.e. residential, commercial, industrial and public) and therefore, damages inflicted to other kind of assets such as road networks, airports, electric systems and other facilities are not considered.

As shown in Table 1, with NP1, the estimated direct losses correspond to almost 4% of the total exposed value of the country whereas for NP2, those same loses are equal to 2.8% of the overall exposed value.

Table 1. Comparison of losses using the two nodal plane solutions for the Guatemala 1976 earthquake

Fault plane	Direct losses (M USD)	Relative loss
NP1	$ 6,717	3.98%
NP2	$ 4,739	2.81%

Besides the difference in the overall modelled damage, it is worth highlighting that the geographical distribution of the damages differs significantly between the two NPs, an issue that has relevance in rapid post-event loss assessments focused on emergency management. Figure 4 shows the comparison of the geographical distribution for the modelled losses after having chosen the two reported NPs.

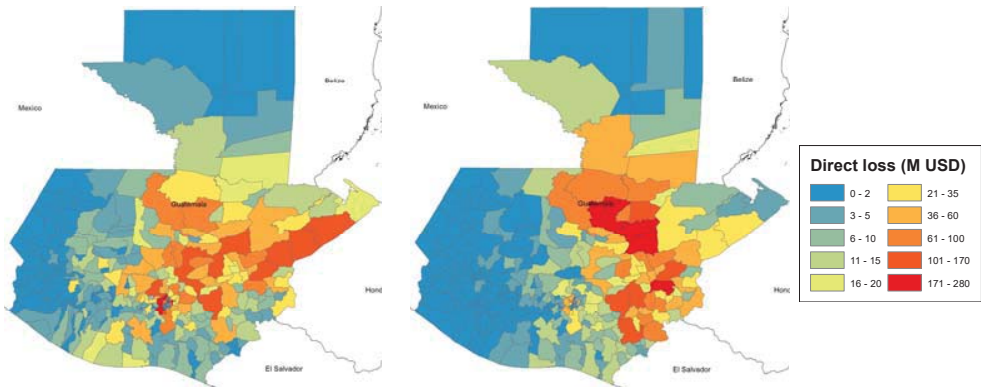

Fig. 4 – Comparison of the geographical distribution of the modelled losses with NP1 (left) and NP2 (right) for the 1976 Guatemala Mw7.5 earthquake

5. Conclusions

We have developed a set of rules to choose in an almost real-time manner the fault plane, knowing the two nodal planes from the centroid moment tensor solution. These rules have been developed based on physical considerations and the observed data. The rules, generally, work and return the desired fault plane. However, as illustrated by the 2005 intraslab earthquake (M_w 7.8) of Terrapaca in northern Chile, in some cases the true fault plane may not be the expected one, resulting in the wrong choice of a nodal plane as the fault plane. Perhaps this happens more often for earthquakes in subducted-slab seismic provinces because of local stresses caused by flexure and distortion of the subducted plate.

Apart from possible wrong choice of the fault plane, mislocation of the event is another source of error in the rapid estimation of seismic intensity and the resulting losses. For example, Singh and Lermo [22] and Hjörleifsdóttir et al. [23] report that the locations of Mexican earthquakes reported by international agencies are systematically mislocated by about 35 km to the NE. Similar, systematic, mislocations are likely for most of the regions. This would cause a spatial shift in the seismic-intensity contours.

In a rapid estimation scenario, the only available source parameters are the location, the two nodal planes and the magnitude. Here, we are obliged to ignore possible source directivity and to estimate the fault dimension from the magnitude with some constrains from prior knowledge of source characteristics in the seismic province. In spite of the errors caused by these approximations, we find that the correct choice of the fault plane provides a significant improvement in the estimations of seismic intensities and losses.

6. References

[1] Ordaz M, Martinelli F, Aguilar A, Arboleda J, Meletti C. and D'Amico V. (2019). R-CRISIS, Program for computing seismic hazard. Instituto de Ingeniería. Universidad Nacional Autónoma de México. Mexico City, Mexico.

[2] Aki K. and Richards P.G. (1981). *Quantitative Seismology*, Volume 1, W.H. Freeman and Company, San Francisco.

[3] Storchak D.A., Di Giacomo D., Bondár I., Engdahl E.R., Harris J., Lee W.H.K., Villaseñor A. and Bormann P. (2013). Public Release of the ISC-GEM Global Instrumental Earthquake Catalogue (1900-2009). Seismological Research Letters. 84(5):810-815.

[4] Salgado-Gálvez M.A., Ordaz M., Singh S.K., Cardona O.D., Reinoso E., Aguado A., Zuloaga D., Huerta B. and Bernal G. (2018). Homogeneous and continuous probabilistic seismic hazard model for Latin America and the Caribbean. Proceedings of the 16th European Conference on Earthquake Engineering. Thessaloniki, Greece.

[5] Pérez-Rocha L.E. and Ordaz M. (2008). Maxima earthquakes for seismic design of structures. Proceedings of the 14th World Conference on Earthquake Engineering. Beijing, China.

[6] Bozzoni F., Corigliano M., Lai C.G., Salazar W., Scandella L., Zuccolo E., Latchman J., Lynch and Robertson R. (2011). Probabilistic seismic hazard assessment at the Eastern Caribbean Islands. Bulletin of the Seismological Society of America. 101(5):2499-2521.

[7] Salazar W., Brown L. and Mannette G. (2013). Probabilistic seismic hazard assessment of Jamaica. Journal of Civil Engineering and Architecture. 7(9):1118-1140.

[8] Alvarado G.E., Benito B., Staller A., Climent A., Camacho E., Rojas W., Marroquín G., Molina E., Talavera J.E., Martínez-Cuevas S. and Lindholm C. (2017). The new Central American seismic hazard zonation: Mutual consensus based in up to day seismotectonic framework. Tectonophysics. 721:462-476.

[9] Plafker G. (1976). Tectonic aspects of the Guatemala earthquake of 4 February 1976, Science. 193, 1201-1208.

[10] Pacheco J. F. and Singh S.K. (2010). Seismicity and state of stress in Guerrero segment of the 490 Mexican subduction zone. Journal of Geophysical Research. 115, B01303.

[11] Melgar D., Ruiz-Angulo A., Soliman García E., Manea M., Xu X., Ramírez-Herrera M.T., Zavala-Hidalgo J., Geng J., Corona N., Pérez-Campos X., Cabral-Cano E. and Ramírez-Guzmán L. (2018). Deep embrittlement and complete rupture of the lithosphere during the Mw 8.2 Tehuantepec earthquake, Nature Geoscience. 11:955–960.

[12] Mirwald A., Cruz-Atienza V.M., Díaz-Mojica J., Iglesias A., Singh S.K., Villafuerte C. and Tago J. (2019). The September 19, 2017 (M_W7.1), intermediate-depth Mexican earthquake: a slow and energetically inefficient deadly shock. Geophysical Research Letters. 46(4):2054-2064.

[13] Peyrat S., Campos J., de Chabalier J.B., Perez A., Bonvalot S., Bouin M.P., Legrand D., Nercessian A., Charade O, Patau G, Clévédé E., Kausel E., Bernard P, Vilotte J.P. (2006). Tarapacá intermediate-depth earthquake (M_W 7.7, 2005, northern Chile): A slab-pull event with horizontal fault plane constrained from seismologic and geodetic observations. Geophysical Research Letters. 33, L22308, doi:10.1029/2006GL027710.

[14] Delouis B. and Legrand D. (2007). M_W 7.8 Tarapaca intermediate depth earthquake of 13 June 2005 (northern Chile): Fault plane identification and slip distribution by waveform inversion, Geophysical Research Letters. 34, L01304, doi:10.1029/2006GL028193.

[15] Kanamori H. and Stewart G.S. (1978). Seismological aspects of the Guatemala earthquake of February 4, 1976, Journal of Geophysical Research. 83(B7):3427-3434.

[16] Wells L. and Coppersmith K.J. (1994). New Empirical Relationships among Magnitude, Rupture Length, Rupture Width, Rupture Area, and Surface Displacement. Bulletin of the Seismological Society of America. 84:974-1002.

[17] Chiou B. and Youngs R. (2014). Update of the Chiou and Youngs NGA Model for the Average Horizontal Component of Peak Ground Motion and Response Spectra. Earthquake Spectra. 30:1117-1153.

[18] United Nations Office for Disaster Risk Reduction – UNISDR (2015). Global Assessment Report on Disaster Risk Reduction. Geneva, Switzerland.

[19] De Bono A. and Chatenoux B. (2015). A global exposure model for GAR 2015. Background paper for GAR15. Geneva, Switzerland.

[20] Ordaz M. (2000). Metodología para la evaluación del riesgo sísmico enfocada a la gerencia de seguros por terremoto. Universidad Nacional Autónoma de México. Mexico City, Mexico.

[21] Salgado-Gálvez M.A., Zuloaga Romero D., Velásquez C.A., Carreño M.L., Cardona O.D. and Barbat A.H. (2016). Urban seismic risk index for Medellín, Colombia, based on probabilistic loss and casualties estimations. Natural Hazards. 80:1995-2021.

[22] Singh S.K. and Lermo J. (1985). Mislocation of Mexican earthquakes as reported in international bulletins, Geofísica Internacional. 24:333-351.

[23] Hjörleifsdóttir V., Singh S.K., and Husker A. (2016). Differences in epicentral location of Mexican earthquakes between local and global catalogs: an update, Geofísica Internacional. 55:79–93.

